sumed, the increase in the rate constant is more significant and the product $r = kc_A$ is *larger* inside the pellet. Because the effectiveness factor compares the actual rate in the pellet to the rate at the surface conditions, it is possible for the effectiveness factor to exceed unity in a nonisothermal pellet, which we see in Figure 7.19.

A second striking feature of the nonisothermal pellet is that multiple steady states are possible. Consider the case $\Phi = 0.01$, $\beta = 0.4$ and $\gamma = 30$ shown in Figure 7.19. The effectiveness factor has three possible values for this case. We show in Figures 7.20 and 7.21 the solution to Equation 7.74 for this case. The three temperature and concentration profiles correspond to an ignited steady state (C), an extinguished steady state (A), and an unstable intermediate steady state (B). As we showed in Chapter 6, whether we achieve the ignited or extinguished steady state in the pellet depends on how the reactor is started. Aris provides further discussion of these cases and shows that many steady-state solutions are possible in some cases [3, p. 51]. For realistic values of the catalyst thermal conductivity, however, the pellet can often be considered isothermal and the energy balance can be neglected [17]. Multiple steady-state solutions in the particle may still occur in practice, however, if there is a large external heat transfer resistance.

7.6 Multiple Reactions

As the next step up in complexity, we consider the case of multiple reactions. Some analytical solutions are available for simple cases with multiple reactions, and Aris provides a comprehensive list [2], but the scope of these is limited. We focus on numerical computation as a general method for these problems. Indeed, we find that even numerical solution of some of these problems is challenging for two reasons. First, steep concentration profiles often occur for realistic parameter values, and we wish to compute these profiles accurately. It is not unusual for species concentrations to change by 10 orders of magnitude within the pellet for realistic reaction and diffusion rates. Second, we are solving boundary-value problems because the boundary conditions are provided at the center and exterior surface of the pellet. Boundary-value problems (BVPs) are generally much more difficult to solve than initial-value problems (IVPs).

A detailed description of numerical methods for this problem is out of place here. We use the collocation method, which is described in more detail in Appendix A. The next example involves five species,

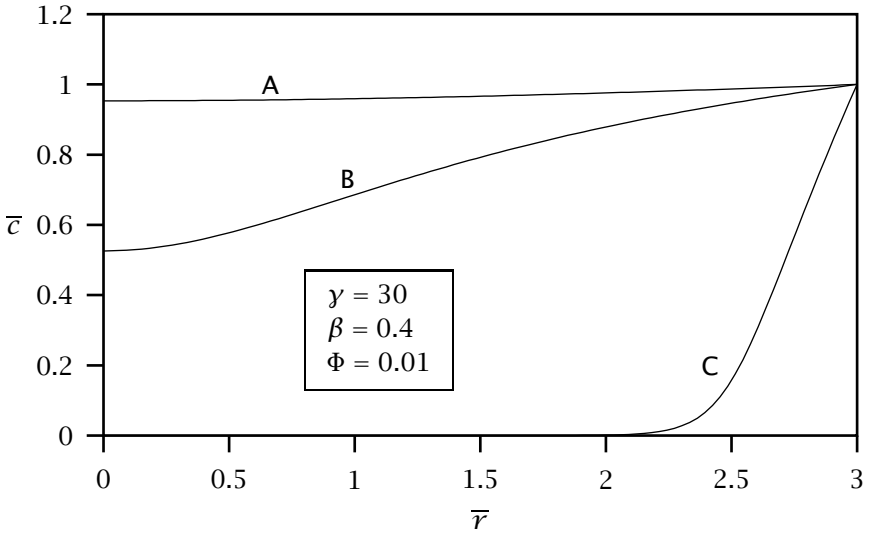

Figure 7.20: Dimensionless concentration versus radius for the non-isothermal spherical pellet: lower (A), unstable middle (B), and upper (C) steady states.

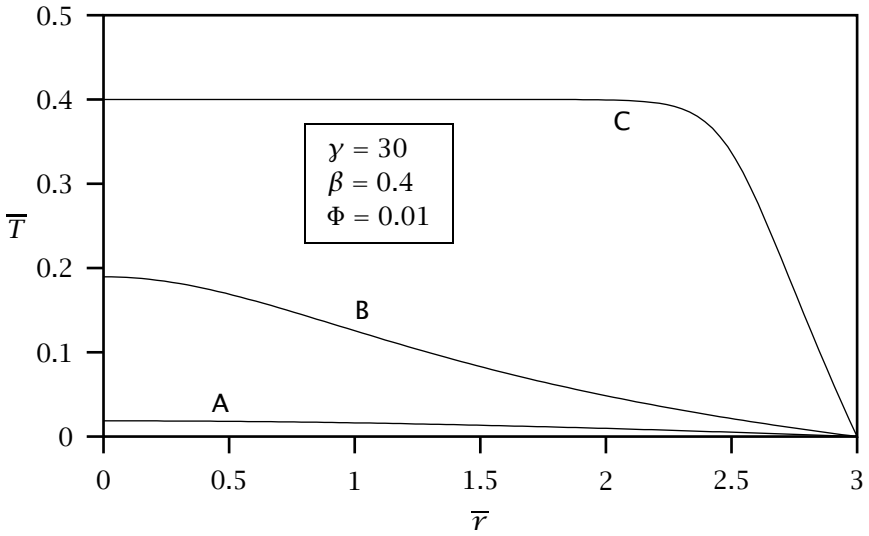

Figure 7.21: Dimensionless temperature versus radius for the non-isothermal spherical pellet: lower (A), unstable middle (B), and upper (C) steady states.

two reactions with Hougen-Watson kinetics, and both diffusion and external mass-transfer limitations.

Example 7.2: Catalytic converter

Consider the oxidation of CO and a representative volatile organic such as propylene in a automobile catalytic converter containing spherical catalyst pellets with particle radius 0.175 cm. The particle is surrounded by a fluid at 1.0 atm pressure and 550 K containing 2% CO, 3% O_2 and 0.05% (500 ppm) C_3H_6. The reactions of interest are

$$CO + \frac{1}{2}O_2 \longrightarrow \quad CO_2 \tag{7.77}$$

$$C_3H_6 + \frac{9}{2}O_2 \longrightarrow 3CO_2 + 3H_2O \tag{7.78}$$

with rate expressions given by Oh et al. [16]

$$r_1 = \frac{k_1 c_{CO} c_{O_2}}{(1 + K_{CO} c_{CO} + K_{C_3H_6} c_{C_3H_6})^2} \tag{7.79}$$

$$r_2 = \frac{k_2 c_{C_3H_6} c_{O_2}}{(1 + K_{CO} c_{CO} + K_{C_3H_6} c_{C_3H_6})^2} \tag{7.80}$$

The rate constants and the adsorption constants are assumed to have Arrhenius form. The parameter values are given in Table 7.5 [16]. The mass-transfer coefficients are taken from DeAcetis and Thodos [9]. The pellet may be assumed to be isothermal. Calculate the steady-state pellet concentration profiles of all reactants and products.

Solution

We solve the steady-state mass balances for the three reactant species,

$$D_j \frac{1}{r^2} \frac{d}{dr} \left(r^2 \frac{dc_j}{dr} \right) = -R_j \tag{7.81}$$

with the boundary conditions

$$\frac{dc_j}{dr} = 0 \qquad r = 0 \tag{7.82}$$

$$D_j \frac{dc_j}{dr} = k_{mj} \left(c_{jf} - c_j \right) \qquad r = R \tag{7.83}$$

$j = \{CO, O_2, C_3H_6\}$. The model is solved using the collocation method. The reactant concentration profiles are shown in Figures 7.22 and 7.23.

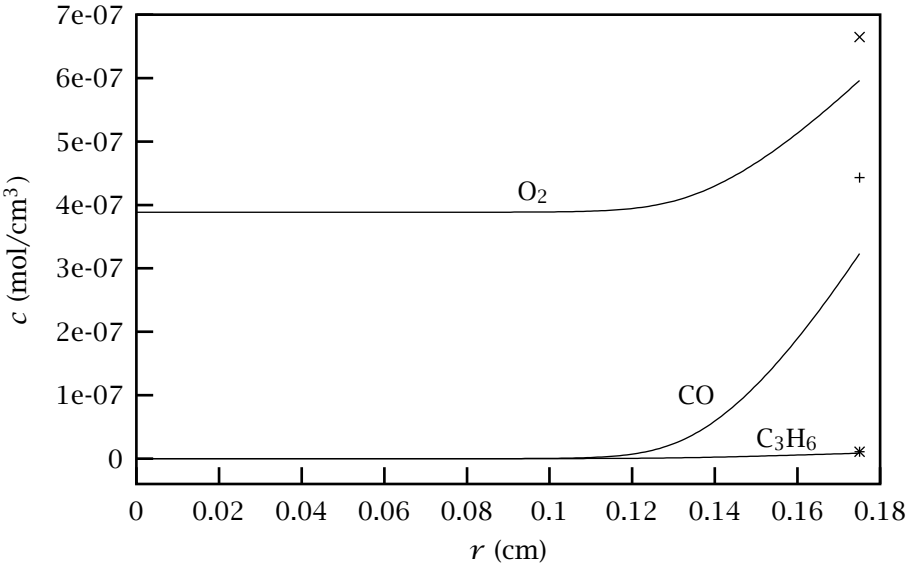

Figure 7.22: Concentration profiles of reactants; fluid concentration of O_2 (×), CO (+), C_3H_6 (∗).

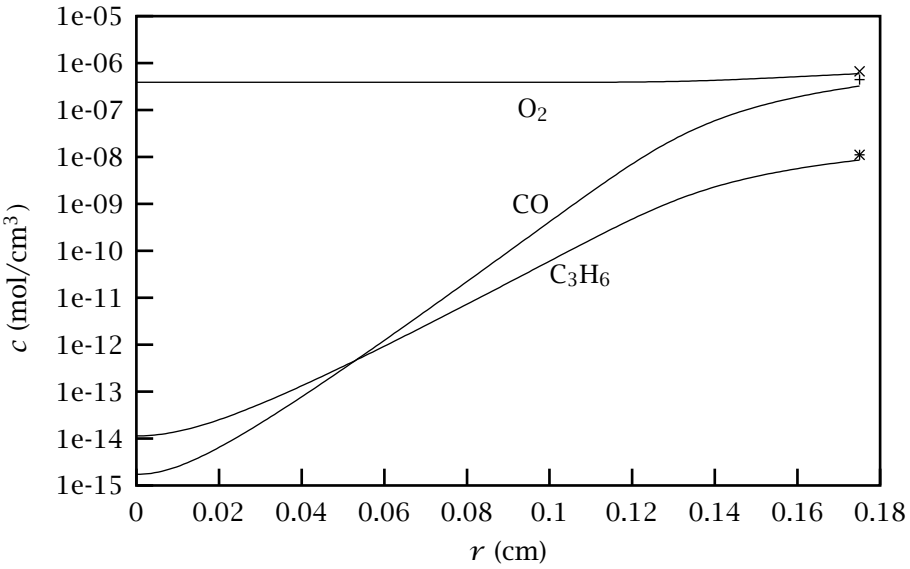

Figure 7.23: Concentration profiles of reactants (log scale); fluid concentration of O_2 (×), CO (+), C_3H_6 (∗).

Parameter	Value	Units	Parameter	Value	Units
P	1.013×10^5	N/m^2	k_{10}	7.07×10^{19}	mol/cm$^3 \cdot$ s
T	550	K	k_{20}	1.47×10^{21}	mol/cm$^3 \cdot$ s
R	0.175	cm	$K_{\mathrm{CO}0}$	8.099×10^6	cm^3/mol
E_1	13,108	K	$K_{\mathrm{C_3H_6}0}$	2.579×10^8	cm^3/mol
E_2	15,109	K	D_{CO}	0.0487	cm^2/s
E_{CO}	−409	K	$D_{\mathrm{O_2}}$	0.0469	cm^2/s
$E_{\mathrm{C_3H_6}}$	191	K	$D_{\mathrm{C_3H_6}}$	0.0487	cm^2/s
$c_{\mathrm{CO}f}$	2.0 %		$k_{m\mathrm{CO}}$	3.90	cm/s
$c_{\mathrm{O_2}f}$	3.0 %		$k_{m\mathrm{O_2}}$	4.07	cm/s
$c_{\mathrm{C_3H_6}f}$	0.05 %		$k_{m\mathrm{C_3H_6}}$	3.90	cm/s

Table 7.5: Kinetic and mass-transfer parameters for the catalytic converter example.

Notice that O_2 is in excess and both CO and C_3H_6 reach very low values within the pellet. The log scale in Figure 7.23 shows that the concentrations of these reactants change by seven orders of magnitude. Obviously the consumption rate is large compared to the diffusion rate for these species. The external mass-transfer effect is noticeable, but not dramatic.

The product concentrations could simply be calculated by solving their mass balances along with those of the reactants. Because we have only two reactions, however, the concentrations of the products are computable from the stoichiometry and the mass balances. If we take the following mass balances

$$\begin{aligned}
D_{\mathrm{CO}}\nabla^2 c_{\mathrm{CO}} &= -R_{\mathrm{CO}} &&= r_1 \\
D_{\mathrm{C_3H_6}}\nabla^2 c_{\mathrm{C_3H_6}} &= -R_{\mathrm{C_3H_6}} &&= r_2 \\
D_{\mathrm{CO_2}}\nabla^2 c_{\mathrm{CO_2}} &= -R_{\mathrm{CO_2}} &&= -r_1 - 3r_2 \\
D_{\mathrm{H_2O}}\nabla^2 c_{\mathrm{H_2O}} &= -R_{\mathrm{H_2O}} &&= -3r_2
\end{aligned}$$

and form linear combinations to eliminate the reaction-rate terms for the two products, we obtain

$$\begin{aligned}
D_{\mathrm{CO_2}}\nabla^2 c_{\mathrm{CO_2}} &= -D_{\mathrm{CO}}\nabla^2 c_{\mathrm{CO}} - 3D_{\mathrm{C_3H_6}}\nabla^2 c_{\mathrm{C_3H_6}} \\
D_{\mathrm{H_2O}}\nabla^2 c_{\mathrm{H_2O}} &= -3D_{\mathrm{C_3H_6}}\nabla^2 c_{\mathrm{C_3H_6}}
\end{aligned}$$

Because the diffusivities are assumed constant, we can integrate these

once on $(0, r)$ to obtain for the products

$$D_{CO_2}\frac{dc_{CO_2}}{dr} = -D_{CO}\frac{dc_{CO}}{dr} - 3D_{C_3H_6}\frac{dc_{C_3H_6}}{dr}$$
$$D_{H_2O}\frac{dc_{H_2O}}{dr} = -3D_{C_3H_6}\frac{dc_{C_3H_6}}{dr}$$

The exterior boundary condition can be rearranged to give

$$c_j - c_{jf} = \frac{D_j}{k_{mj}}\frac{dc_j}{dr}$$

Substituting in the relationships for the products gives

$$c_{CO_2} = c_{CO_2 f} - \frac{1}{k_{mCO_2}}\left[D_{CO}\frac{dc_{CO}}{dr} + 3D_{C_3H_6}\frac{dc_{C_3H_6}}{dr}\right]$$
$$c_{H_2O} = c_{H_2O f} - \frac{1}{k_{mH_2O}}\left[3D_{C_3H_6}\frac{dc_{C_3H_6}}{dr}\right]$$

The right-hand sides are available from the solution of the material balances of the reactants. Plotting these results for the products gives Figure 7.24. We see that CO_2 is the main product. Note the products flow out of the pellet, unlike the reactants shown in Figures 7.22 and 7.23, which are flowing into the pellet. □

7.7 Fixed-Bed Reactor Design

Given our detailed understanding of the behavior of a single catalyst particle, we now are prepared to pack a tube with a bed of these particles and solve the fixed-bed reactor design problem. In the fixed-bed reactor, we keep track of two phases. The fluid-phase streams through the bed and transports the reactants and products through the reactor. The reaction-diffusion processes take place in the solid-phase catalyst particles. The two phases communicate to each other by exchanging mass and energy at the catalyst particle exterior surfaces. We have constructed a detailed understanding of all these events, and now we assemble them together.

7.7.1 Coupling the Catalyst and Fluid

We make the following assumptions:

1. Uniform catalyst pellet exterior. Particles are small compared to the length of the reactor.

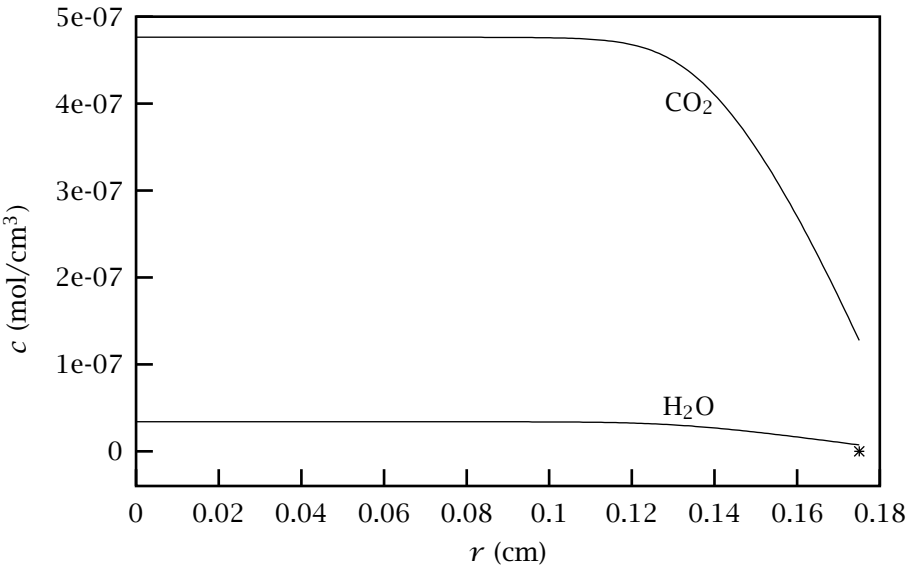

Figure 7.24: Concentration profiles of the products; fluid concentration of CO_2 (×), H_2O (+).

2. Plug flow in the bed, no radial profiles.
3. Neglect axial diffusion in the bed.
4. Steady state.

Fluid. In the fluid phase, we track the molar flows of all species, the temperature and the pressure. We can no longer neglect the pressure drop in the tube because of the catalyst bed. We use an empirical correlation to describe the pressure drop in a packed tube, the well-known Ergun equation [10]. Therefore, we have the following differential equations for the fluid phase

$$\frac{dN_j}{dV} = R_j \tag{7.84}$$

$$Q\rho\hat{C}_p\frac{dT}{dV} = -\sum_i \Delta H_{Ri} r_i + \frac{2}{R}U^o(T_a - T) \tag{7.85}$$

$$\frac{dP}{dV} = -\frac{(1-\epsilon_B)}{D_p\epsilon_B^3}\frac{Q}{A_c^2}\left[150\frac{(1-\epsilon_B)\mu_f}{D_p} + \frac{7}{4}\frac{\rho Q}{A_c}\right] \tag{7.86}$$

The fluid-phase boundary conditions are provided by the known feed conditions at the tube entrance

$$N_j = N_{jf}, \qquad z = 0 \tag{7.87}$$
$$T = T_f, \qquad z = 0 \tag{7.88}$$
$$P = P_f, \qquad z = 0 \tag{7.89}$$

Catalyst particle. Inside the catalyst particle, we track the concentrations of all species and the temperature. We neglect any pressure effect inside the catalyst particle. We have the following differential equations for the catalyst particle

$$D_j \frac{1}{r^2}\frac{d}{dr}\left(r^2 \frac{d\tilde{c}_j}{dr}\right) = -\tilde{R}_j \tag{7.90}$$
$$\hat{k}\frac{1}{r^2}\frac{d}{dr}\left(r^2 \frac{d\tilde{T}}{dr}\right) = \sum_i \Delta H_{Ri}\tilde{r}_i \tag{7.91}$$

The boundary conditions are provided by the mass-transfer and heat-transfer rates at the pellet exterior surface, and the zero slope conditions at the pellet center

$$\frac{d\tilde{c}_j}{dr} = 0 \qquad r = 0 \tag{7.92}$$
$$D_j \frac{d\tilde{c}_j}{dr} = k_{jm}(c_j - \tilde{c}_j) \qquad r = R \tag{7.93}$$
$$\frac{d\tilde{T}}{dr} = 0 \qquad r = 0 \tag{7.94}$$
$$\hat{k}\frac{d\tilde{T}}{dr} = k_T(T - \tilde{T}) \qquad r = R \tag{7.95}$$

Coupling equations. Finally, we equate the production rate R_j experienced by the fluid phase to the production rate inside the particles, which is where the reaction takes place. Analogously, we equate the enthalpy change on reaction experienced by the fluid phase to the enthalpy change on reaction taking place inside the particles. These ex-

pressions are given below

$$\underbrace{R_j}_{\text{rate } j \text{ / vol}} = -\underbrace{(1-\epsilon_B)}_{\text{vol cat / vol}} \underbrace{\frac{S_p}{V_p} D_j \left.\frac{d\widetilde{c}_j}{dr}\right|_{r=R}}_{\text{rate } j \text{ / vol cat}} \tag{7.96}$$

$$\underbrace{\sum_i \Delta H_{Ri} r_i}_{\text{rate heat / vol}} = \underbrace{(1-\epsilon_B)}_{\text{vol cat / vol}} \underbrace{\frac{S_p}{V_p} \hat{k} \left.\frac{d\widetilde{T}}{dr}\right|_{r=R}}_{\text{rate heat / vol cat}} \tag{7.97}$$

Notice we require the bed porosity to convert from the rate per volume of particle to the rate per volume of reactor. The bed porosity or void fraction, ϵ_B, is defined as the volume of voids per volume of reactor. The volume of catalyst per volume of reactor is therefore $1 - \epsilon_B$. This information can be presented in a number of equivalent ways. We can easily measure the density of the pellet, ρ_p, and the density of the bed, ρ_B. From the definition of bed porosity, we have the relation

$$\rho_B = (1 - \epsilon_B)\rho_p$$

or if we solve for the volume fraction of catalyst

$$1 - \epsilon_B = \rho_B / \rho_p$$

Figure 7.25 shows the particles and fluid, and summarizes the coupling relations between the two phases.

Equations 7.84–7.97 provide the full packed-bed reactor model given our assumptions. We next examine several packed-bed reactor problems that can be solved without solving this full set of equations. Finally, we present Example 7.7, which requires numerical solution of the full set of equations.

Example 7.3: First-order, isothermal fixed-bed reactor

Use the rate data presented in Example 7.1 to find the fixed-bed reactor volume and the catalyst mass needed to convert 97% of A. The feed to the reactor is pure A at 1.5 atm at a rate of 12 mol/s. The 0.3 cm pellets are to be used, which leads to a bed density $\rho_B = 0.6$ g/cm^3. Assume the reactor operates isothermally at 450 K and that external mass-transfer limitations are negligible.

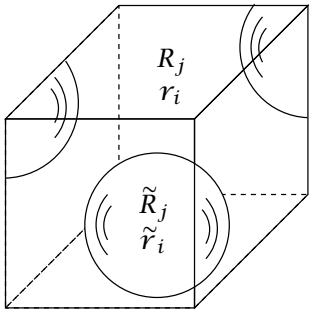

Mass

$$R_j = (1-\epsilon_B)\tilde{R}_{jp}$$

$$\tilde{R}_{jp} = -\frac{S_p}{V_p} D_j \left.\frac{d\tilde{c}_j}{dr}\right|_{r=R}$$

Energy

$$\sum_i \Delta H_{Ri} r_i = (1-\epsilon_B) \sum_i \Delta H_{Ri} \tilde{r}_{ip}$$

$$\sum_i \Delta H_{Ri} \tilde{r}_{ip} = \frac{S_p}{V_p} \hat{k} \left.\frac{d\tilde{T}}{dr}\right|_{r=R}$$

Figure 7.25: Fixed-bed reactor volume element containing fluid and catalyst particles; the equations show the coupling between the catalyst particle balances and the overall reactor balances.

Solution

We solve the fixed-bed design equation

$$\frac{dN_A}{dV} = R_A = -(1-\epsilon_B)\eta k c_A$$

between the limits N_{Af} and $0.03N_{Af}$, in which c_A is the A concentration in the fluid. For the first-order, isothermal reaction, the Thiele modulus is independent of A concentration, and is therefore independent of axial position in the bed

$$\Phi = \frac{R}{3}\sqrt{\frac{k}{D_A}} = \frac{0.3\text{cm}}{3}\sqrt{\frac{2.6\text{s}^{-1}}{0.007\text{cm}^2/\text{s}}} = 1.93$$

The effectiveness factor is also therefore a constant

$$\eta = \frac{1}{\Phi}\left[\frac{1}{\tanh 3\Phi} - \frac{1}{3\Phi}\right] = \frac{1}{1.93}\left[1 - \frac{1}{5.78}\right] = 0.429$$

In Chapter 4, Equation 4.75, we express the concentration of A in terms of molar flows for an ideal-gas mixture

$$c_A = \frac{P}{RT}\left(\frac{N_A}{N_A + N_B}\right)$$

The total molar flow is constant due to the reaction stoichiometry so $N_A + N_B = N_{Af}$ and we have

$$c_A = \frac{P}{RT}\frac{N_A}{N_{Af}}$$

Substituting these values into the material balance, rearranging and integrating over the volume gives

$$V_R = -(1-\epsilon_B)\left(\frac{RTN_{Af}}{\eta kP}\right)\int_{N_{Af}}^{0.03N_{Af}} \frac{dN_A}{N_A}$$

$$V_R = -\left(\frac{0.6}{0.85}\right)\frac{(82.06)(450)(12)}{(0.429)(2.6)(1.5)}\ln(0.03) = 1.32\times 10^6 \text{cm}^3$$

and

$$W_c = \rho_B V_R = \frac{0.6}{1000}\left(1.32\times 10^6\right) = 789 \text{ kg}$$

We see from this example that if the Thiele modulus and effectiveness factors are constant, finding the size of a fixed-bed reactor is no more difficult than finding the size of a plug-flow reactor. □

Example 7.4: Mass-transfer limitations in a fixed-bed reactor

Reconsider Example 7.3 given the following two values of the mass-transfer coefficient

$$k_{m1} = 0.07 \text{ cm/s}$$
$$k_{m2} = 1.4 \text{ cm/s}$$

Solution

First we calculate the Biot numbers from Equation 7.61 and obtain

$$B_1 = \frac{(0.07)(0.1)}{(0.007)} = 1$$
$$B_2 = \frac{(1.4)(0.1)}{(0.007)} = 20$$

Inspection of Figure 7.17 indicates that we expect a significant reduction in the effectiveness factor due to mass-transfer resistance in the first case, and little effect in the second case. Evaluating the effectiveness factors with Equation 7.65 indeed shows

$$\eta_1 = 0.165$$
$$\eta_2 = 0.397$$

which we can compare to $\eta = 0.429$ from the previous example with no mass-transfer resistance. We can then easily calculate the required catalyst mass from the solution of the previous example without mass-transfer limitations, and the new values of the effectiveness factors

$$V_{R1} = \left(\frac{0.429}{0.165}\right)(789) = 2051 \text{ kg}$$
$$V_{R2} = \left(\frac{0.429}{0.397}\right)(789) = 852 \text{ kg}$$

As we can see, the first mass-transfer coefficient is so small that more than twice as much catalyst is required to achieve the desired conversion compared to the case without mass-transfer limitations. The second mass-transfer coefficient is large enough that only 8% more catalyst is required. □

Example 7.5: Second-order, isothermal fixed-bed reactor

Estimate the mass of catalyst required in an isothermal fixed-bed reactor for the second-order, heterogeneous reaction.

$$\text{A} \xrightarrow{\text{k}} \text{B}$$

$$r = kc_A^2 \qquad k = 2.25 \times 10^5 \text{cm}^3/\text{mol s}$$

The gas feed consists of A and an inert, each with molar flowrate of 10 mol/s, the total pressure is 4.0 atm and the temperature is 550 K. The desired conversion of A is 75%. The catalyst is a spherical pellet with a radius of 0.45 cm. The pellet density is $\rho_p = 0.68$ g/cm^3 and the bed density is $\rho_B = 0.60$ g/cm^3. The effective diffusivity of A is 0.008 cm^2/s and may be assumed constant. You may assume the fluid and pellet surface concentrations are equal.

Solution

We solve the fixed-bed design equation

$$\frac{dN_A}{dV} = R_A = -(1-\epsilon_B)\eta k c_A^2$$
$$N_A(0) = N_{Af} \tag{7.98}$$

between the limits N_{Af} and $0.25N_{Af}$. We again express the concentration of A in terms of the molar flows

$$c_A = \frac{P}{RT}\left(\frac{N_A}{N_A + N_B + N_I}\right)$$

As in the previous example, the total molar flow is constant and we know its value at the entrance to the reactor

$$N_T = N_{Af} + N_{Bf} + N_{If} = 2N_{Af}$$

Therefore,

$$c_A = \frac{P}{RT}\frac{N_A}{2N_{Af}} \tag{7.99}$$

Next we use the definition of Φ for nth-order reactions given in Equation 7.47

$$\Phi = \frac{R}{3}\left[\frac{(n+1)kc_A^{n-1}}{2D_e}\right]^{1/2} = \frac{R}{3}\left[\frac{(n+1)k}{2D_e}\left(\frac{P}{RT}\frac{N_A}{2N_{Af}}\right)^{n-1}\right]^{1/2} \tag{7.100}$$

Substituting in the parameter values gives

$$\Phi = 9.17\left(\frac{N_A}{2N_{Af}}\right)^{1/2} \tag{7.101}$$

For the second-order reaction, Equation 7.101 shows that Φ varies with the molar flow, which means Φ and η vary along the length of the reactor as N_A decreases. We are asked to estimate the catalyst mass needed to achieve a conversion of A equal to 75%. So for this particular example, Φ decreases from 6.49 to 3.24. As shown in Figure 7.9, we can *approximate* the effectiveness factor for the second-order reaction using the analytical result for the first-order reaction, Equation 7.42,

$$\eta = \frac{1}{\Phi}\left[\frac{1}{\tanh 3\Phi} - \frac{1}{3\Phi}\right] \tag{7.102}$$

Summarizing so far, to compute N_A versus V_R, we solve one differential equation, Equation 7.98, in which we use Equation 7.99 for c_A, and Equations 7.101 and 7.102 for Φ and η. We march in V_R until $N_A = 0.25N_{Af}$. The solution to the differential equation is shown in Figure 7.26. The required reactor volume and mass of catalyst are:

$$V_R = 361 \text{ L}, \qquad W_c = \rho_B V_R = 216 \text{ kg}$$

As a final exercise, given that Φ ranges from 6.49 to 3.24, we can make the large Φ approximation

$$\eta = \frac{1}{\Phi} \tag{7.103}$$

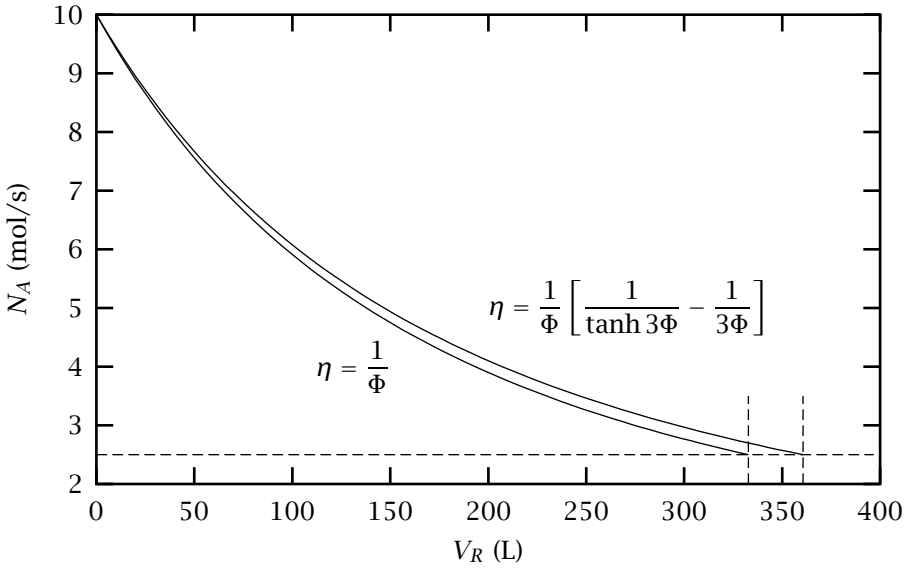

Figure 7.26: Molar flow of A versus reactor volume for second-order, isothermal reaction in a fixed-bed reactor.

to obtain a closed-form solution. If we substitute this approximation for η, and Equation 7.100 into Equation 7.98 and rearrange we obtain

$$\frac{dN_A}{dV} = \frac{-(1-\epsilon_B)\sqrt{k}\,(P/RT)^{3/2}}{(R/3)\sqrt{3/D_A}(2N_{Af})^{3/2}} N_A^{3/2}$$

Separating and integrating this differential equation gives

$$V_R = \frac{4\left[(1-x_A)^{-1/2} - 1\right] N_{Af}(R/3)\sqrt{3/D_A}}{(1-\epsilon_B)\sqrt{k}\,(P/RT)^{3/2}} \qquad (7.104)$$

Large Φ approximation

The results for the large Φ approximation also are shown in Figure 7.26. Notice from Figure 7.9 that we are slightly overestimating the value of η using Equation 7.103, so we underestimate the required reactor volume. The reactor size and the percent change in reactor size are

$$V_R = 333 \text{ L}, \qquad \Delta = -7.7\%$$

Given that we have a result valid for all Φ that requires solving only a single differential equation, one might question the value of this closed-

form solution. One advantage is purely practical. We may not have a computer available. Instructors are usually thinking about in-class examination problems at this juncture. The other important advantage is insight. It is not readily apparent from the differential equation what would happen to the reactor size if we double the pellet size, or halve the rate constant, for example. Equation 7.104, on the other hand, provides the solution's dependence on all parameters. As shown in Figure 7.26 the approximation error is small. Remember to check that the Thiele modulus is large for the entire tube length, however, before using Equation 7.104. □

Example 7.6: Hougen-Watson kinetics in a fixed-bed reactor

The following reaction converting CO to CO_2 takes place in a catalytic, fixed-bed reactor operating isothermally at 838 K and 1.0 atm

$$CO + \frac{1}{2}O_2 \longrightarrow CO_2 \tag{7.105}$$

The following rate expression and parameters are adapted from a different model given by Oh et al. [16]. The rate expression is assumed to be of the Hougen-Watson form

$$r = \frac{k c_{CO} c_{O_2}}{1 + K c_{CO}} \qquad \text{mol/s cm}^3 \text{ pellet}$$

The constants are provided below

$$\begin{aligned} k &= 8.73 \times 10^{12} \exp(-13,500/T) \text{ cm}^3/\text{mol s} \\ K &= 8.099 \times 10^{6} \exp(409/T) \text{ cm}^3/\text{mol} \\ D_{CO} &= 0.0487 \text{ cm}^2/\text{s} \end{aligned}$$

in which T is in Kelvin. The catalyst pellet radius is 0.1 cm. The feed to the reactor consists of 2 mol% CO, 10 mol% O_2, zero CO_2 and the remainder inerts. Find the reactor volume required to achieve 95% conversion of the CO.

Solution

Given the reaction stoichiometry and the excess of O_2, we can neglect the change in c_{O_2} and approximate the reaction as pseudo-first order

in CO

$$r = \frac{k' c_{CO}}{1 + K c_{CO}} \qquad \text{mol/s cm}^3 \text{ pellet}$$
$$k' = k c_{O_2 f}$$

which is of the form analyzed in Section 7.4.4. We can write the mass balance for the molar flow of CO,

$$\frac{dN_{CO}}{dV} = -(1 - \epsilon_B)\eta r(c_{CO})$$

in which c_{CO} is the fluid CO concentration. From the reaction stoichiometry, we can express the remaining molar flows in terms of N_{CO}

$$N_{O_2} = N_{O_2 f} + 1/2(N_{CO} - N_{CO f})$$
$$N_{CO_2} = N_{CO f} - N_{CO}$$
$$N = N_{O_2 f} + 1/2(N_{CO} + N_{CO f})$$

The concentrations follow from the molar flows assuming an ideal-gas mixture

$$c_j = \frac{P}{RT}\frac{N_j}{N}$$

To decide how to approximate the effectiveness factor shown in Figure 7.14, we evaluate $\phi = K_{C0} c_{C0}$, at the entrance and exit of the fixed-bed reactor. With ϕ evaluated, we compute the Thiele modulus given in Equation 7.58 and obtain

$$\phi = 32.0 \qquad \Phi = 79.8, \qquad \text{entrance}$$
$$\phi = 1.74 \qquad \Phi = 326, \qquad \text{exit}$$

It is clear from these values and Figure 7.14 that $\eta = 1/\Phi$ is an excellent approximation for this reactor. Substituting this equation for η into the mass balance and solving the differential equation produces the results shown in Figure 7.27. The concentration of O_2 is nearly constant, which justifies the pseudo-first-order rate expression. Reactor volume

$$V_R = 233 \text{ L}$$

is required to achieve 95% conversion of the CO. Recall that the volumetric flowrate varies in this reactor so conversion is based on molar flow, not molar concentration. Figure 7.28 shows how Φ and ϕ vary with position in the reactor. □

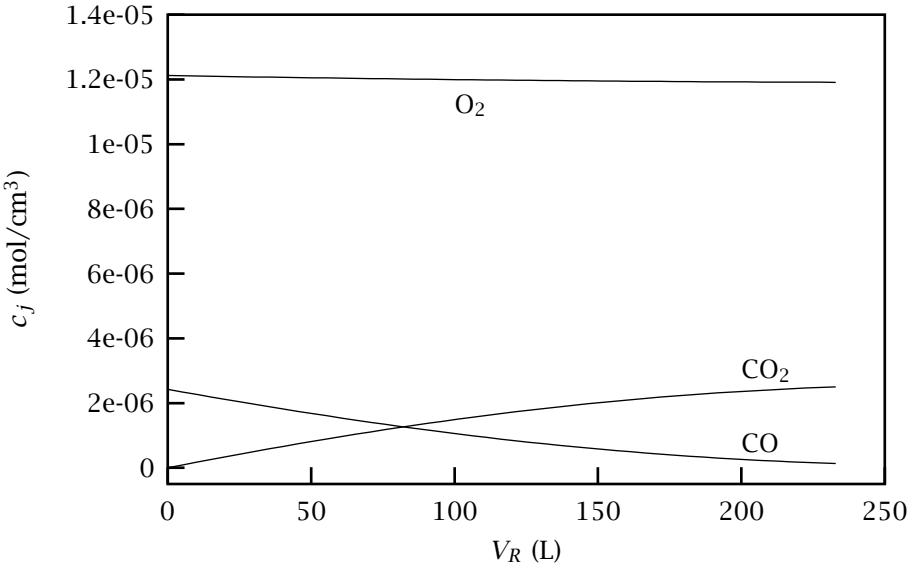

Figure 7.27: Molar concentrations versus reactor volume.

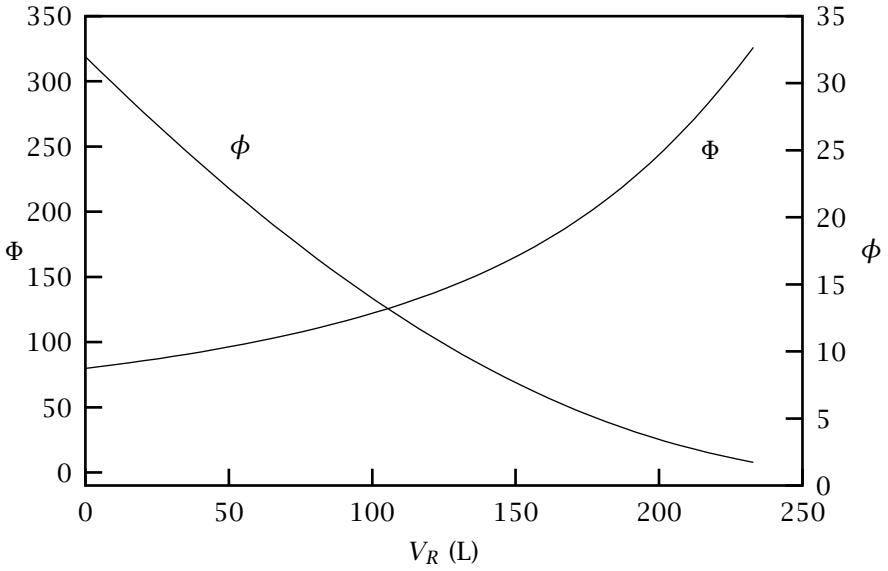

Figure 7.28: Dimensionless equilibrium constant and Thiele modulus versus reactor volume. Values indicate $\eta = 1/\Phi$ is a good approximation for entire reactor.

Parameter	Value	Units
P_f	2.02×10^5	N/m^2
T_f	550	K
R_t	5.0	cm
u_f	75	cm/s
T_a	325	K
U^o	5.5×10^{-3}	cal/(cm^2 Ks)
ΔH_{R1}	-67.63×10^3	cal/(mol CO K)
ΔH_{R2}	-460.4×10^3	cal/(mol C_3H_6 K)
$\hat{C}_p$	0.25	cal/(g K)
μ_f	0.028×10^{-2}	g/(cm s)
ρ_b	0.51	g/cm^3
ρ_p	0.68	g/cm^3

Table 7.6: Feed flowrate and heat-transfer parameters for the fixed-bed catalytic converter.

In the previous examples, we have exploited the idea of an effectiveness factor to reduce fixed-bed reactor models to the same form as plug-flow reactor models. This approach is useful and solves several important cases, but this approach is also limited and can take us only so far. In the general case, we must contend with multiple reactions that are not first order, nonconstant thermochemical properties, and nonisothermal behavior in the pellet and the fluid. For these cases, we have no alternative but to solve numerically for the temperature and species concentrations profiles in both the pellet and the bed. As a final example, we compute the numerical solution to a problem of this type.

We use the collocation method to solve the next example, which involves five species, two reactions with Hougen-Watson kinetics, both diffusion and external mass-transfer limitations, and nonconstant fluid temperature, pressure and volumetric flowrate.

Example 7.7: Multiple-reaction, nonisothermal fixed-bed reactor

Evaluate the performance of the catalytic converter in converting CO and propylene. Determine the amount of catalyst required to convert 99.6% of the CO and propylene. The reaction chemistry and pellet mass-transfer parameters are given in Table 7.5. The feed conditions and heat-transfer parameters are given in Table 7.6.

Solution

The fluid balances govern the change in the fluid concentrations, temperature and pressure. The pellet concentration profiles are solved with the collocation approach. The pellet and fluid concentrations are coupled through the mass-transfer boundary condition. The fluid concentrations are shown in Figure 7.29. A bed volume of 1098 cm^3 is required to convert the CO and C_3H_6. Figure 7.29 also shows that oxygen is in slight excess.

The reactor temperature and pressure are shown in Figure 7.30. The feed enters at 550 K, and the reactor experiences about a 130 K temperature rise while the reaction essentially completes; the heat losses then reduce the temperature to less than 500 K by the exit. The pressure drops from the feed value of 2.0 atm to 1.55 atm at the exit. Notice the catalytic converter exit pressure of 1.55 atm must be large enough to account for the remaining pressure drops in the tail pipe and muffler.

In Figures 7.31 and 7.32, the pellet CO concentration profile at several reactor positions is displayed. The feed profile, marked by ① in Figure 7.32, is similar to the one shown in Figure 7.23 of Example 7.2 (the differences are caused by the different feed pressures). We see that as the reactor heats up, the reaction rates become large and the CO is rapidly converted inside the pellet. By 490 cm^3 in the reactor, the pellet exterior CO concentration has dropped by two orders of magnitude, and the profile inside the pellet has become very steep. As the reactions go to completion and the heat losses cool the reactor, the reaction rates drop. At 890 cm^3, the CO begins to diffuse back into the pellet. Finally, the profiles become much flatter near the exit of the reactor.

It can be numerically challenging to calculate rapid changes and steep profiles inside the pellet. The good news, however, is that accurate pellet profiles are generally *not* required for an accurate calculation of the overall pellet reaction rate. The reason is that when steep profiles are present, essentially all of the reaction occurs in a thin shell near the pellet exterior. We can calculate accurately down to concentrations on the order of 10^{-15} as shown in Figure 7.32, and by that point, essentially zero reaction is occurring, and we can calculate an accurate overall pellet reaction rate. It is always a good idea to vary the numerical approximation in the pellet profile, by changing the number of collocation points, to ensure convergence in the fluid profiles. □

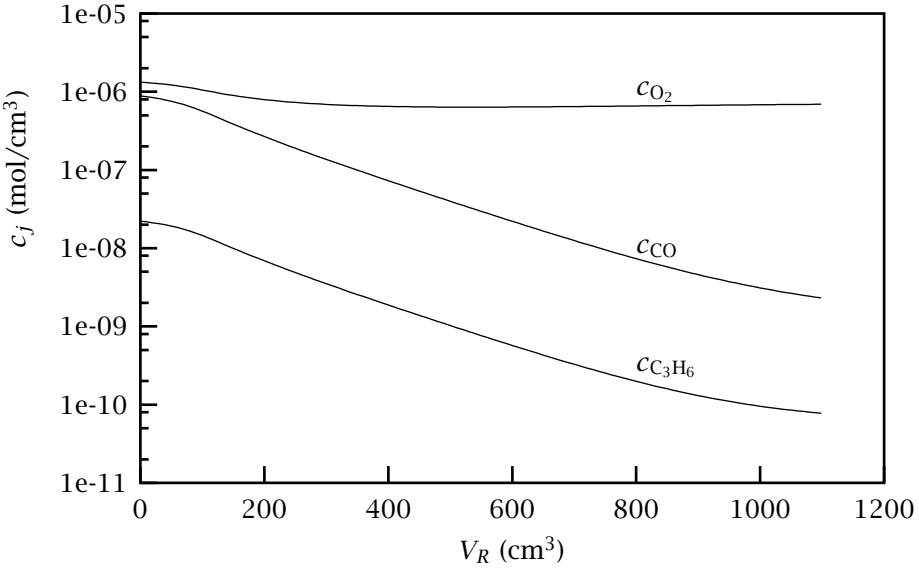

Figure 7.29: Fluid molar concentrations versus reactor volume.

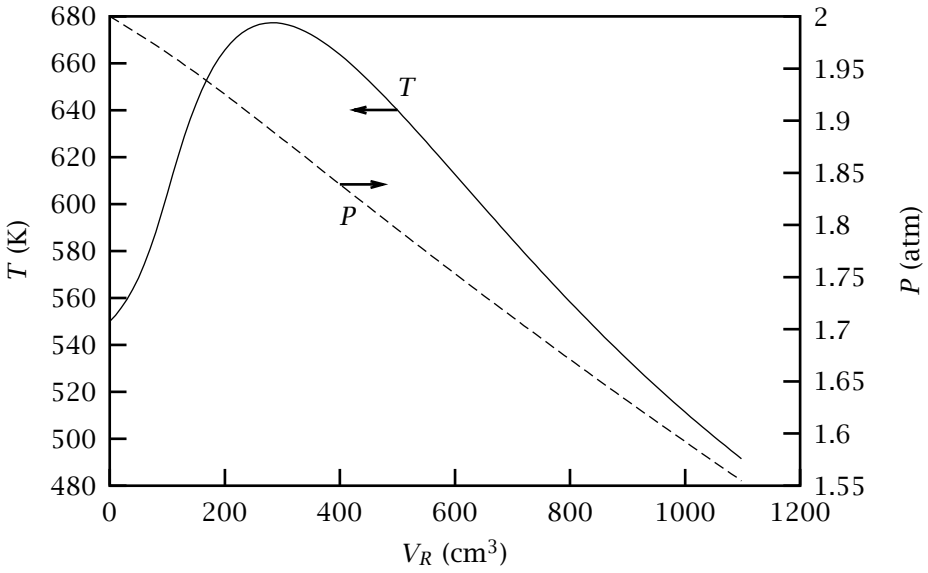

Figure 7.30: Fluid temperature and pressure versus reactor volume.

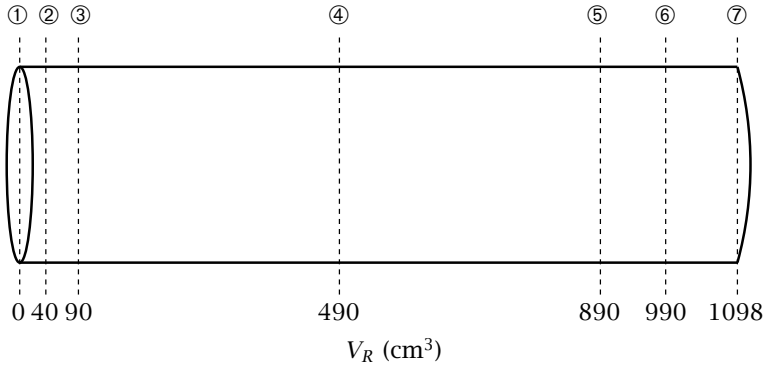

Figure 7.31: Reactor positions for pellet profiles.

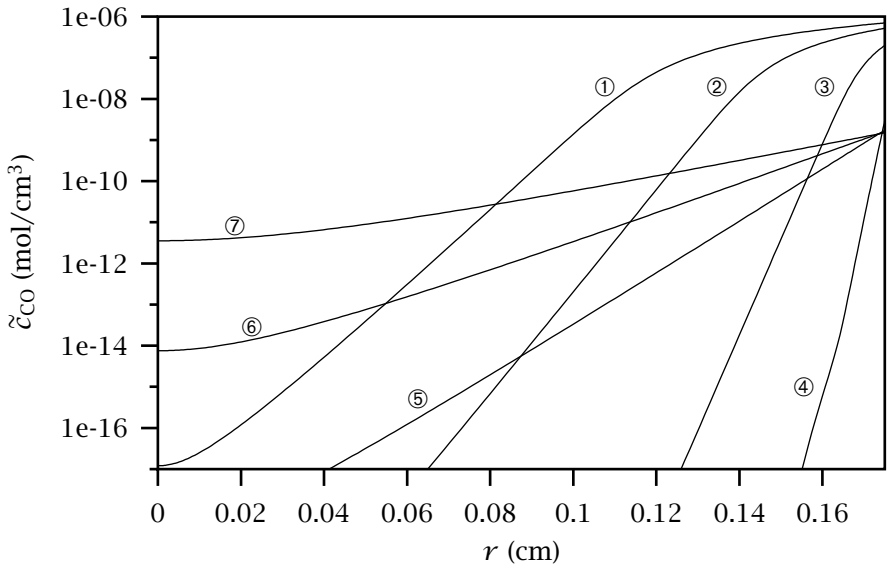

Figure 7.32: Pellet CO profiles at several reactor positions.